COMPARISON BETWEEN THE FIRST ORDER UPWIND UNSTRUCTURED ALGORITHMS OF ROE AND OF HARTEN IN THE SOLUTION OF THE EULER EQUATIONS IN TWO-DIMENSIONS

Edisson Sávio de Góes Maciel, saviomaciel@pq.cnpq.br
CNPq Researcher – Rua Demócrito Cavalcanti, 152 – Afogados – Recife – PE – Brazil – 50750-080

Abstract. *The present work performs comparisons between the Roe and the Harten algorithms applied to the solution of aeronautical and of aerospace problems, in two-dimensions. The Euler equations in conservative form, employing a finite volume formulation and an unstructured spatial discretization, are solved. Both schemes are flux difference splitting ones and accurate solutions are expected. The time integration is performed by a Runge-Kutta method of five stages. Both schemes are first order accurate in space and second order accurate in time. The steady state physical problems of the transonic flow along a convergent-divergent nozzle and of the supersonic flows along a ramp and around a blunt body are studied. In all problems, the value of the entrance or attack angle is considered equal to zero. A spatially variable time step procedure is implemented aiming to accelerate the convergence of the schemes to the steady state condition. The results have demonstrated that the Roe scheme presents more severe pressure fields in the ramp and blunt body problems and a more accurate value of the stagnation pressure in the blunt body case than the Harten scheme.*

Keywords: *Roe algorithm, Harten algorithm, Flux difference splitting schemes, Euler equations, Two-dimensions.*

1. INTRODUCTION

Conventional non-upwind algorithms have been used extensively to solve a wide variety of problems (Kutler, 1975, and Steger, 1978). Conventional algorithms are somewhat unreliable in the sense that for every different problem (and sometimes, every different case in the same class of problems) artificial dissipation terms must be specially tuned and judicially chosen for convergence. Also, complex problems with shocks and steep compression and expansion gradients may defy solution altogether.

Upwind schemes are in general more robust but are also more involved in their derivation and application. Some upwind schemes that have been applied to the Euler equations are: Roe (1981) and Harten (1983). Some comments about these methods are reported below:

Roe (1981) presented a work that emphasized that several numerical schemes to the solution of the hyperbolic conservation equations were based on exploring the information obtained in the solution of a sequence of Riemann problems. It was verified that in the existent schemes the major part of these information was degraded and that only certain solution aspects were solved. It was demonstrated that the information could be preserved by the construction of a matrix with a certain "U property". After the construction of this matrix, its eigenvalues could be considered as wave velocities of the Riemann problem and the U_L-U_R projections over the matrix's eigenvectors would be the jumps which occur between intermediate stages.

Harten (1983) developed a class of new finite difference schemes, explicit and with second order of spatial accuracy to calculation of weak solutions of the hyperbolic conservation laws. These schemes highly non-linear were obtained by the application of a first order non-oscillatory scheme to an appropriated modified flux function. The so derived second order schemes reached high resolution, while preserved the robustness property of the original non-oscillatory first order scheme.

On an unstructured algorithm context, Maciel (2005a) and Maciel (2005b) have presented works involving the numerical implementation of two typical algorithms of the Computational Fluid Dynamics community. The Jameson and Mavriplis (1986) and the Frink, Parikh and Pirzadeh (1991) algorithms were implemented on an unstructured spatial discretization context. The Jameson and Mavriplis (1986) scheme was symmetrical and the Mavriplis (1990) artificial dissipation operator was implemented aiming to guarantee the scheme stability. The Frink, Parikh and Pirzadeh (1991) scheme was upwind and of flux difference splitting type based on Roe (1981) method. The Jameson and Mavriplis (1986) scheme was second order accurate in space and time, while the Frink, Parikh and Pirzadeh (1991) scheme was first order accurate in space and second order accurate in time. The Euler equations in conservative form were solved. The physical problems of the transonic flow around a NACA 0012 airfoil and the supersonic flow around a simplified version of the VLS (Brazilian Satellite Launcher Vehicle) were studied and good results were obtained, highlighting better solution quality and convergence acceleration features to the Jameson and Mavriplis (1986) scheme.

In the present work, the Roe (1981) and the Harten (1983) schemes are implemented, on a finite volume context and using an upwind and unstructured spatial discretization, to solve the Euler equations in the two-dimensional space applied to the steady state physical problems of the transonic flow along a convergent-divergent nozzle and of the supersonic flows along a ramp and around a blunt body. The Roe (1981) and the Harten (1983) schemes are flux difference splitting ones and accurate solutions are expected. The implemented schemes are first order accurate in

space. The time integration uses a Runge-Kutta method and is second order accurate. Both algorithms are accelerated to the steady state solution using a spatially variable time step. This technique has proved excellent gains in terms of convergence ratio as reported in Maciel (2005c). The results have demonstrated that the Roe (1981) scheme presents more severe pressure fields in the ramp and blunt body problems and a more accurate value of the stagnation pressure in the blunt body case than the Harten (1983) scheme.

An unstructured discretization of the calculation domain is usually recommended to complex configurations, due to the easily and efficiency that such domains can be discretized (Mavriplis, 1990, and Pirzadeh, 1991). However, the unstructured mesh generation question will not be studied in this work.

2. EULER EQUATIONS

The fluid movement is described by the Euler equations, which express the conservation of mass, of linear momentum and of energy to an inviscid mean, heat non-conductor and compressible, in the absence of external forces. In integral and conservative forms, these equations can be represented by:

$$\partial/\partial t \int_V Q dV + \int_S \left[(E_e) n_x + (F_e) n_y \right] dS = 0 \,, \tag{1}$$

with Q written to a Cartesian system, V is the cell volume, n_x and n_y are the components of the normal versor to the flux face, S is the flux area, and E_e and F_e are the convective flux vector components. The Q, E_e and F_e vectors are represented by:

$$Q = \begin{Bmatrix} \rho \\ \rho u \\ \rho v \\ e \end{Bmatrix}, \quad E_e = \begin{Bmatrix} \rho u \\ \rho u^2 + p \\ \rho uv \\ (e+p)u \end{Bmatrix} \quad and \quad F_e = \begin{Bmatrix} \rho v \\ \rho uv \\ \rho v^2 + p \\ (e+p)v \end{Bmatrix}, \tag{2}$$

being ρ the fluid density; u and v the Cartesian components of the velocity vector in the x and y directions, respectively; e the total energy per fluid volume unity; and p the static pressure of the fluid mean.

In the nozzle problem, the Euler equations were nondimensionalized in relation to the stagnation density and in relation to the critical speed of sound. In the others problems, the nondimensionalization is performed considering freestream density and freestream speed of sound. The matrix system of the Euler equations is closed with the state equation $p = (\gamma - 1)\left[e - 0.5\rho(u^2 + v^2) \right]$, assuming the ideal gas hypothesis. The total enthalpy is determined by $H = (e + p)/\rho$.

3. ROE (1981) ALGORITHM

The Roe (1981) algorithm, first order accurate in space, is specified by the determination of the numerical flux vector at "*l*" interface.

Following a finite volume formalism, which is equivalent to a generalized coordinate system, the right and left cell volumes, as well the interface volume, necessary to a coordinate change, are defined by:

$$V_R = V_{ne}\,, \quad V_L = V_i \quad \text{and} \quad V_l = 0.5(V_R + V_L)\,, \tag{3}$$

where "*R*" and "*L*" represent right and left states, respectively, and "*ne*" represent a neighbor volume to the "*i*" volume. The subscript "*L*" is associated to properties of a given "*i*" cell and the subscript "*R*" is associated to properties of the "*ne*" neighbor cell of "*i*". The cell volume on an unstructured context is defined by:

$$V_i = 0.5\left| (x_{n1} y_{n2} + y_{n1} x_{n3} + x_{n2} y_{n3}) - (x_{n3} y_{n2} + y_{n3} x_{n1} + x_{n2} y_{n1}) \right|, \tag{4}$$

with n_1, n_2 and n_3 being the nodes of a given triangular cell. The area components at the "*l*" interface are defined by:

$$S_x^l = n_x^l S^l \quad \text{and} \quad S_y^l = n_y^l S^l \,, \tag{5}$$

where n_x^l, n_y^l and S^l are defined as:

$$n_x^l = \Delta y_l \Big/ \left(\Delta x_l^2 + \Delta y_l^2\right)^{0.5},\ n_y^l = -\Delta x_l \Big/ \left(\Delta x_l^2 + \Delta y_l^2\right)^{0.5} \quad \text{and} \quad S^l = \left(\Delta x_l^2 + \Delta y_l^2\right)^{0.5}. \tag{6}$$

Expressions to Δx_l and Δy_l are given in Tab. 1. Figure 1 illustrates the "*i*" volume and its respective neighbors, its nodes and its flux interfaces.

Table 1. Values of Δx_l and Δy_l.

Interface	Δx_l	Δy_l
$l = 1$	$x_{n2} - x_{n1}$	$y_{n2} - y_{n1}$
$l = 2$	$x_{n3} - x_{n2}$	$y_{n3} - y_{n2}$
$l = 3$	$x_{n1} - x_{n3}$	$y_{n1} - y_{n3}$

The metric terms to this generalized coordinate system are defined as:

$$h_x = S_x^l / V_l,\ h_y = S_y^l / V_l \quad \text{and} \quad h_n = S^l / V_l. \tag{7}$$

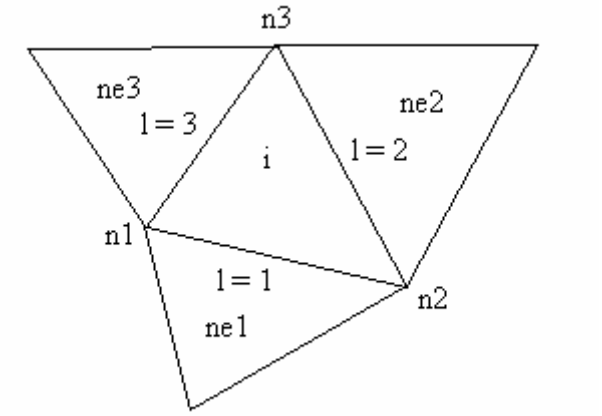

Figure 1. Schematic of a cell and its neighbors, nodes and flux interfaces.

The properties calculated at the flux interface are obtained by arithmetical average or by Roe (1981) average. In the present work, the Roe (1981) average was used:

$$\rho_l = \sqrt{\rho_L \rho_R},\ u_l = \left(u_L + u_R\sqrt{\rho_R/\rho_L}\right) \Big/ \left(1 + \sqrt{\rho_R/\rho_L}\right),\ v_l = \left(v_L + v_R\sqrt{\rho_R/\rho_L}\right) \Big/ \left(1 + \sqrt{\rho_R/\rho_L}\right); \tag{8}$$

$$H_l = \left(H_L + H_R\sqrt{\rho_R/\rho_L}\right) \Big/ \left(1 + \sqrt{\rho_R/\rho_L}\right) \quad \text{and} \quad a_l = \sqrt{(\gamma - 1)\left[H_l - 0.5\left(u_l^2 + v_l^2\right)\right]}. \tag{9}$$

The eigenvalues of the Euler equations, in the normal direction to the flux face, to the convective flux are given by:

$$q_{normal} = u_l h_x + v_l h_y,\ \lambda_1 = q_{normal} - a_l h_n,\ \lambda_2 = \lambda_3 = q_{normal} \quad \text{and} \quad \lambda_4 = q_{normal} + a_l h_n. \tag{10}$$

The jumps of the conserved variables, necessary to the construction of the Roe (1981) dissipation function, are given by:

$$\Delta e = V_l\left(e_R - e_L\right),\ \Delta\rho = V_l\left(\rho_R - \rho_L\right),\ \Delta(\rho u) = V_l\left[(\rho u)_R - (\rho u)_L\right] \text{ and } \Delta(\rho v) = V_l\left[(\rho v)_R - (\rho v)_L\right]; \tag{11}$$

The α vectors to the "*l*" interface are calculated by the following expressions:

$$\alpha_1 = 0.5(aa - bb),\ \alpha_2 = \Delta\rho - aa,\ \alpha_3 = cc \quad \text{and} \quad \alpha_4 = 0.5(aa + bb), \tag{12}$$

with:

$$aa = (\gamma - 1)/a_l^2 \left[\Delta e + 0.5\left(u_l^2 + v_l^2\right)\Delta\rho - u_l\Delta(\rho u) - v_l\Delta(\rho v)\right]; \tag{13}$$

$$bb = 1/a_l \left[h_x^{'}\Delta(\rho u) - \left(h_x^{'}u_l + h_y^{'}v_l\right)\Delta\rho + h_y^{'}\Delta(\rho v)\right]; \tag{14}$$

$$cc = h_x^{'}\Delta(\rho v) + \left(h_y^{'}u_l - h_x^{'}v_l\right)\Delta\rho - h_y^{'}\Delta(\rho u); \tag{15}$$

$$h_x^{'} = h_x/h_n \quad \text{and} \quad h_y^{'} = h_y/h_n\ . \tag{16}$$

The Roe (1981) dissipation function is constructed using the following matrix:

$$R_l = \begin{bmatrix} 1 & 1 & 0 & 1 \\ u_l - h_x^{'}a_l & u_l & -h_y^{'} & u_l + h_x^{'}a_l \\ v_l - h_y^{'}a_l & v_l & h_x^{'} & v_l + h_y^{'}a_l \\ H_l - h_x^{'}u_l a_l - h_y^{'}v_l a_l & 0.5\left(u_l^2 + v_l^2\right) & h_x^{'}v_l - h_y^{'}u_l & H_l + h_x^{'}u_l a_l + h_y^{'}v_l a_l \end{bmatrix}. \tag{17}$$

The entropy condition is implemented of the following way:

$$\psi_m = \begin{cases} |\lambda_m|, & if\ |\lambda_m| \geq \varepsilon_m \\ 0.5\left(\lambda_m^2 + \varepsilon_m^2\right)/\varepsilon_m, & if\ |\lambda_m| < \varepsilon_m \end{cases} \text{ to non-linear fields and } \psi_m = |\lambda_m| \text{ to linear fields,} \tag{18}$$

with "*m*" assuming values 1 and 4 to non-linear fields and 2 and 3 to linear fields, ε_m assuming the value 0.2, recommended by Roe (1981).

Finally, the Roe (1981) dissipation function to the "*l*" interface is constructed by the following matrix-vector product:

$$\{D_{Roe}\}_l = [R]_l \{-\psi\alpha\}_l\ . \tag{19}$$

The convective numerical flux vector to the "*l*" interface is described by:

$$F_l^{(m)} = \left(E_l^{(m)}h_x + F_l^{(m)}h_y\right)V_l + 0.5D_{Roe}^{(m)}, \text{ with: } E_l^{(m)} = 0.5\left(E_R^{(m)} + E_L^{(m)}\right) \text{ and } F_l^{(m)} = 0.5\left(F_R^{(m)} + F_L^{(m)}\right). \tag{20}$$

The time integration is performed by an explicit method, second order accurate, Runge-Kutta type of five stages and can be represented of generalized form by:

$$\begin{aligned} Q_i^{(0)} &= Q_i^{(n)} \\ Q_i^{(k)} &= Q_i^{(0)} - \alpha_k\, \Delta t_i / V_i \times C\left(Q_i^{(k-1)}\right), \\ Q_i^{(n+1)} &= Q_i^{(k)} \end{aligned} \tag{21}$$

with k = 1,...,5; α_1 = 1/4, α_2 = 1/6, α_3 = 3/8, α_4 = 1/2 and α_5 = 1. The contribution of the convective numerical flux vectors is determined by the C_i vector:

$$C_i^{(m)} = F_1^{(m)} + F_2^{(m)} + F_3^{(m)}\ . \tag{22}$$

4. HARTEN (1983) ALGORITHM

The Harten (1983) algorithm, first order accurate in space, is specified by the determination of the numerical flux vector at "*l*" interface. This scheme uses Equations (3) to (17) of Roe (1981) scheme, also using the Roe (1981) average to determine the interface properties. The next step consists in determining the entropy condition. The entropy condition is implemented of the following way:

$$\upsilon_m = \Delta t\lambda_m = Z_m \quad \text{and} \quad \psi_m = \begin{cases} |Z_m|, & if\ |Z_m| \geq \delta_f \\ 0.5\left(Z_m^2 + \delta_f^2\right)/\delta_f, & if\ |Z_m| < \delta_f \end{cases}, \tag{23}$$

with "m" varying from 1 to 4 (two-dimensional space) and δ_f assuming values between 0.1 and 0.5, being 0.2 the value suggested by Harten (1983).

The Harten (1983) dissipation function to the "l" interface is constructed by the following matrix-vector product:

$$\{D_{Harten}\}_l = [R]_l \left\{ -\psi\alpha \Big/ \Delta t_i \right\}_l . \tag{24}$$

The convective numerical flux vector to the "l" interface is described by:

$$F_l^{(m)} = \left(E_l^{(m)} h_x + F_l^{(m)} h_y\right) V_l + 0.5 D_{Harten}^{(m)} , \tag{25}$$

with $E_l^{(m)}$ and $F_l^{(m)}$ defined according to Eq. (20). The time integration is performed by the Runge-Kutta explicit method, second order accurate, of five stages, described in Eq. (21). The contribution of the convective numerical flux vectors is determined by the C_i vector:

$$C_i^{(m)} = F_1^{(m)} + F_2^{(m)} + F_3^{(m)} . \tag{26}$$

5. SPATIALLY VARIABLE TIME STEP

The basic idea of this procedure consists in keeping constant the CFL number in all calculation domain, allowing, hence, the use of appropriated time steps to each specific mesh region during the convergence process. Hence, according to the definition of the CFL number, it is possible to write:

$$\Delta t_i = CFL(\Delta s)_i / c_i , \tag{27}$$

where CFL is the "Courant-Friedrichs-Lewy" number to provide numerical stability to the scheme; $c_i = \left[\left(u^2 + v^2\right)^{0.5} + a\right]_i$ is the maximum characteristic velocity of information propagation in the calculation domain; and $(\Delta s)_i$ is a characteristic length of information transport. On a finite volume context, $(\Delta s)_i$ is chosen as the minor value found between the minor centroid distance, involving the "i" cell and a neighbor, and the minor cell side length.

6. INITIAL AND BOUNDARY CONDITIONS

Stagnation values are used as initial condition to the nozzle problem (Maciel, 2002). Only at the exit boundary is imposed a reduction of 1/3 to the density and to the pressure to start the flow along the nozzle. To the others problems, values of freestream flow are adopted for all properties as initial condition, in the whole calculation domain (Jameson and Mavriplis, 1986, Maciel, 2005a, Maciel, 2005b, and Maciel, 2002). To a detailed description of these initial conditions, see Maciel (2007).

The boundary conditions are basically of three types: solid wall, entrance and exit. These conditions are implemented in special cells named ghost cells. Details of the present implementation are described in Maciel (2007).

7. RESULTS

Tests were performed in a CELERON - 1.2 GHz and 640 Mbytes of RAM memory microcomputer. Converged results occurred to four (4) orders of reduction in the value of the maximum residue. The maximum residue is defined as the maximum value obtained from the discretized conservation equations. The value used for γ was 1.4. To all problems, the entrance or attack angle adopted a value 0.0°.

Table 2. Data of the unstructured meshes.

	Nozzle	Ramp	Blunt body
	61x71	61x100	103x100
Cells	8,400	11,880	20,196
Nodes	4,331	6,100	10,300

The meshes used in the simulations were structured generated, using rectangular cells, and posteriorly were transformed in meshes of triangles through specific subroutines implemented in the calculation algorithms, where the connectivity,

neighboring, node coordinate and ghost cell tables were generated to the simulations. On this context, only the advantages of unstructured meshes were not appreciated; however, the unstructured algorithms could be tested on a context of unstructured spatial discretization. Table 2 shows the data of the generated meshes. The second line indicates the mesh data on a finite difference context.

7.1. Nozzle physical problem

The geometry of the convergent-divergent nozzle is described in Fig. 2. The total length of the nozzle is 0.38ft (0.116m) and the throat height is equal to 0.090ft (0.027m). The throat is located at 0.19ft (0.058m) from the entrance boundary. The throat curvature ratio is equal to 0.090ft. The nozzle convergence angle is 22.33° and the nozzle divergence angle is 1.21°. An exponential stretching of 10% in both ξ and η directions was used. The mesh employed to this problem is described in Tab. 2.

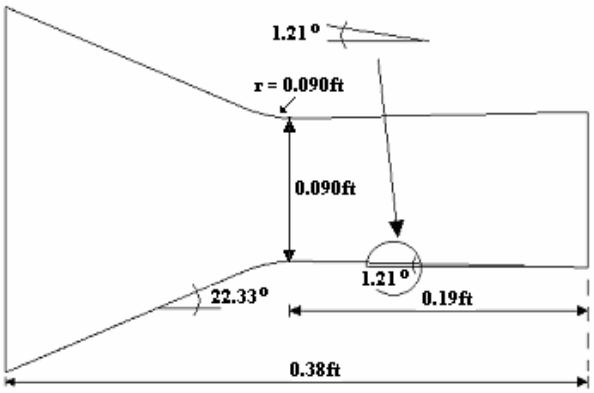

Figure 2. Nozzle configuration.

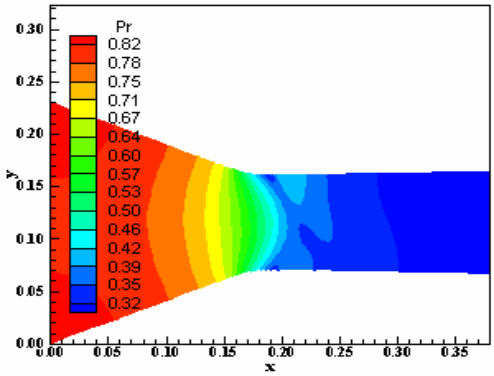

Figure 3. Pressure contours (R).

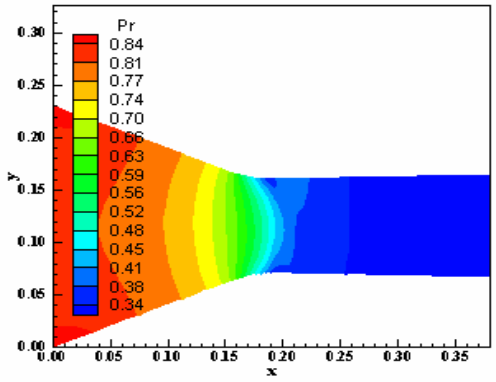

Figure 4. Pressure contours (H).

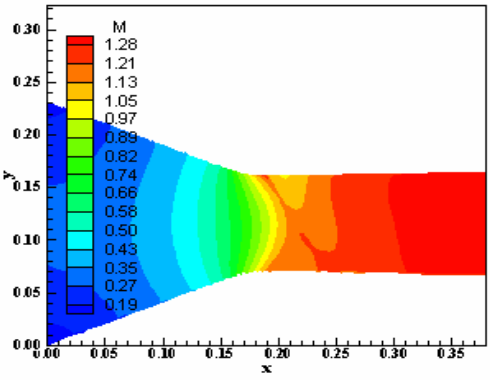

Figure 5. Mach number contours (R).

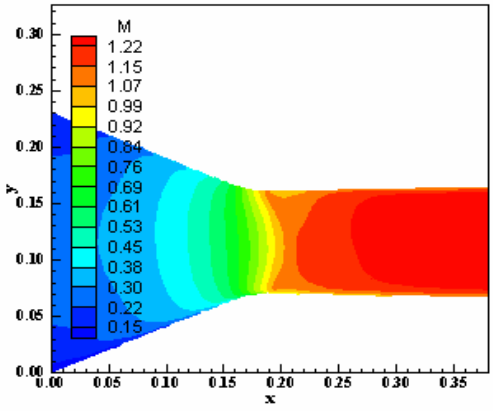

Figure 6. Mach number contours (H).

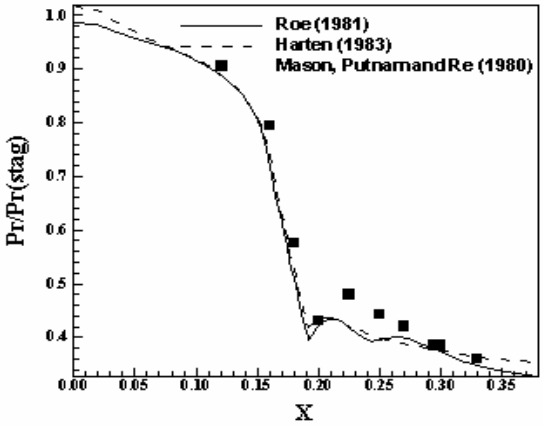

Figure 7. Lower wall pressure distributions.

Figures 3 and 4 show the pressure contours obtained by the Roe (1981) and by the Harten (1983) schemes, respectively. Loss of symmetry is observed in both solutions at the throat region. The pressure field generated by the Harten (1983) scheme is more severe than that generated by the Roe (1981) scheme. Figures 5 and 6 exhibit the Mach number contours obtained by the Roe (1981) and by the Harten (1983) schemes, respectively. Loss of symmetry is again observed in both solutions. The Mach number field generated by the Roe (1981) scheme is more intense than that generated by the Harten (1983) scheme. Figure 7 exhibits the nozzle lower wall pressure distributions obtained by the Roe (1981) and by the Harten (1983) schemes. These pressure distributions are compared with the experimental results of Mason, Putnam and Re (1980). The Harten (1983) solution is closer to the experimental results.

7.2. Ramp physical problem

The ramp configuration is described in Fig. 8. The mesh employed to this problem is described in Tab. 2. The initial condition adopted for this problem was a freestream Mach number of 2.0, characterizing a supersonic flow.

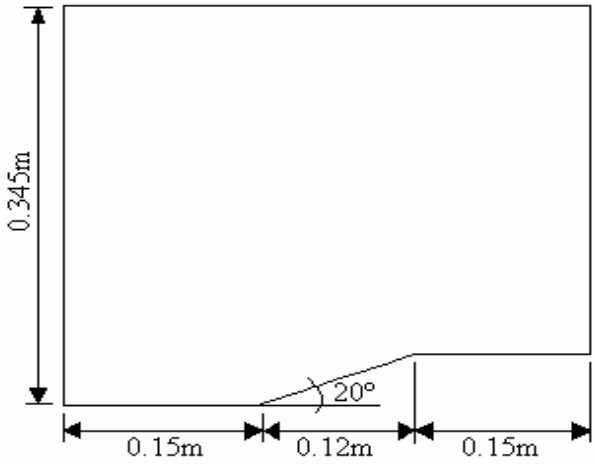

Figure 8. Ramp configuration.

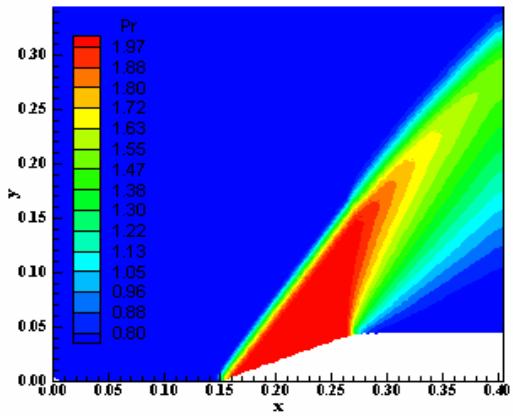

Figure 9. Pressure contours (R).

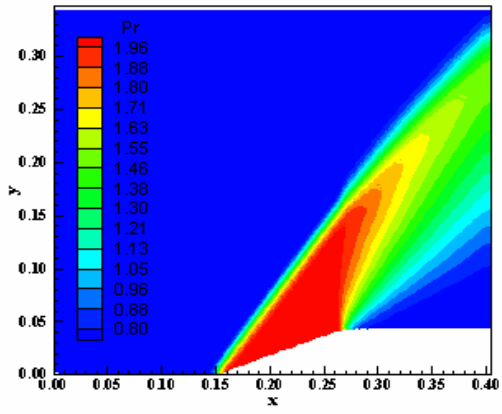

Figure 10. Pressure contours (H).

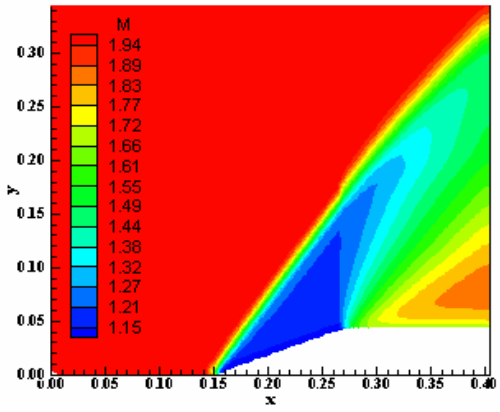

Figure 11. Mach number contours (R).

Figures 9 and 10 show the pressure contours obtained by the Roe (1981) and by the Harten (1983) schemes, respectively. The pressure field generated by the Roe (1981) scheme is more severe than the Harten (1983) ones. In both solutions the shock is well captured. Figures 11 to 12 exhibit the Mach number contours obtained by the Roe (1981) and by the Harten (1983) schemes, respectively. Both Mach number fields are practically identical in quantitative and qualitative terms. Figure 13 shows the ramp pressure distributions obtained by both schemes. They are compared with the oblique shock wave and the Prandtl-Meyer expansion theories. As can be observed, both schemes slightly overpredict the pressure plateau generated by the shock at the ramp in comparison with the theory results. The same behavior is noted in the prediction of the pressure after the expansion fan. Both schemes slightly overpredict this pressure. Even so, the results are of good quality and the Roe (1981) and the Harten (1983) schemes capture appropriately the shock and the expansion fan.

One way to quantitatively verify if the solutions generated by each scheme are satisfactory consists in determining the shock angle of the oblique shock wave, β, measured in relation to the initial direction of the flow field. Anderson Jr. (1984) presents a diagram with values of the shock angle, β, to oblique shock waves. The value of this angle is specified

as function of the freestream Mach number and of the deflection angle of the flow after the shock wave, ϕ.

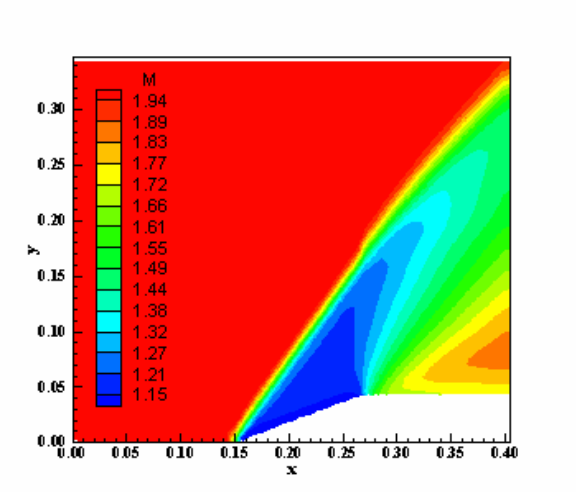

Figure 12. Mach number contours (H).

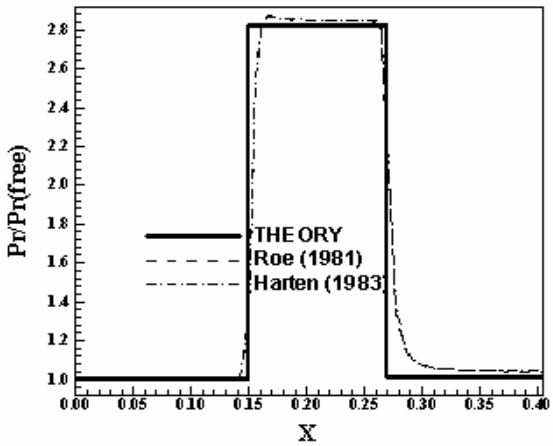

Figure 13. Wall pressure distributions.

To ϕ = 20º (ramp inclination angle) and to a freestream Mach number equals to 2.0, it is possible to obtain from this diagram a value to β equals to 53.0º. Using a transfer in Figures 9 and 10, it is possible to obtain the values of β to each scheme, as well the respective errors, shown in Tab. 3. Both schemes predict the same shock angle.

Table 3. Shock angle and percentage errors to the ramp problem.

Algorithm:	β (°):	Error (%):
Roe (1981)	54.5	2.8
Harten (1983)	54.5	2.8

7.3. Blunt body physical problem

Figure 14 shows the blunt body configuration. The entrance boundary was positioned at 20 times the curvature ratio of the blunt body nose in relation to the blunt body nose. The mesh employed to this problem is described in Tab. 2. The freestream flow Mach number adopted for this simulation was 3.0, characterizing a supersonic flow regime.

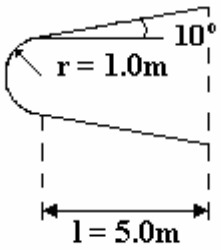

Figure 14. Blunt body configuration.

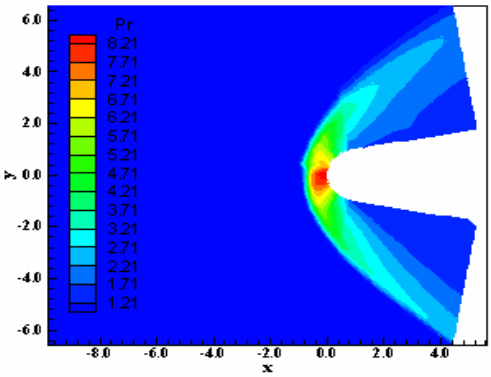

Figure 15. Pressure contours (R).

Figures 15 and 16 exhibit the pressure contours obtained by the Roe (1981) and by the Harten (1983) schemes, respectively. Good symmetry properties are observed in both solutions in opposite behavior as observed in the nozzle problem. The Roe (1981) scheme presents some problems at the blunt body nose. The Roe (1981) scheme presents more severe pressure field than the Harten (1983) scheme. Figures 17 and 18 show the Mach number contours obtained by the Roe (1981) and by the Harten (1983) schemes. Good symmetry properties are again observed, except the Roe (1981) solution at the blunt body nose, and the shock is appropriately captured. Figure 19 exhibits the –Cp distributions around the blunt body wall obtained by both schemes. They present similar –Cp distributions. The Roe (1981) scheme presents some oscillations at x = 0.5m. The small divergence involving the solutions occurs at x = 1.0m, but the Cp peak at the shock is equal to both schemes and the constant pressure plateau after x = 1.0m, the rectilinear wall blunt body region, is well captured after 1.5m.

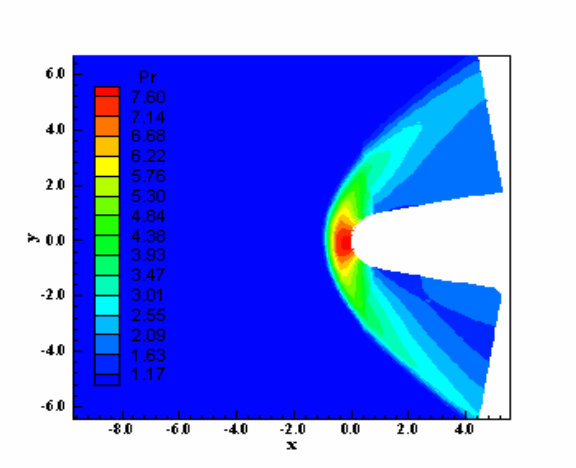

Figure 16. Pressure contours (H).

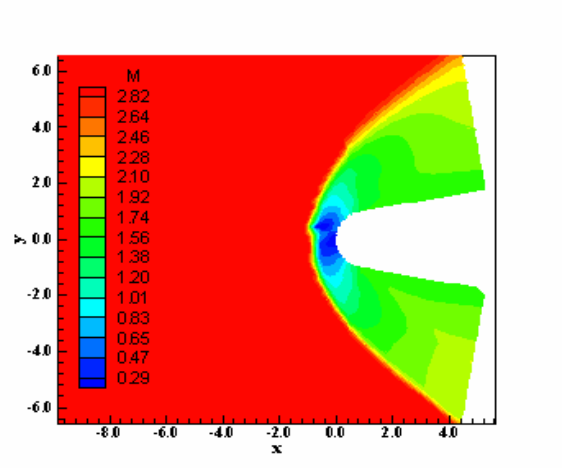

Figure 17. Mach number contours (R).

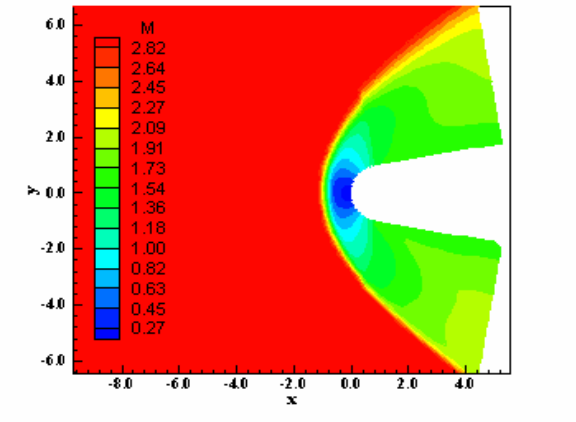

Figure 18. Mach number contours (H).

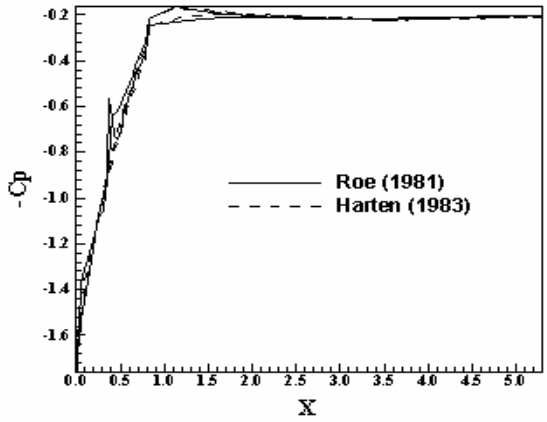

Figure 19. Wall –Cp distributions.

Another possibility to quantitative comparison of all schemes is the determination of the stagnation pressure ahead of the configuration. Anderson Jr. (1984) presents a table of normal shock wave properties in its B Appendix. This table permits the determination of some shock wave properties as function of the freestream Mach number. In front of the blunt body configuration, the shock wave presents a normal shock behavior, which permits the determination of the stagnation pressure, behind the shock wave, from the tables encountered in Anderson Jr. (1984). It is possible to determine the ratio pr_0/pr_∞ from Anderson Jr. (1984), where pr_0 is the stagnation pressure in front of the configuration and pr_∞ is the freestream pressure (equals to $1/\gamma$ with the present nondimensionalization).

Hence, to this problem, $M_\infty = 3.0$ corresponds to $pr_0/pr_\infty = 12.06$ and remembering that $pr_\infty = 0.714$, it is possible to conclude that $pr_0 = 8.61$. Values of the stagnation pressure, with respective percentage errors, to each scheme are shown in Tab. 4. The best result is obtained with the Roe (1981) scheme, with minor percentage error.

Table 4. Values of the stagnation pressure and percentage errors.

Algorithm:	pr_0:	Error (%):
Roe (1981)	8.21	4.6
Harten (1983)	7.60	11.7

7.4. Numerical data of the simulations

Table 5. CFL numbers, iterations to convergence and computational costs of the schemes.

	Nozzle		Ramp		Blunt body		
Scheme	CFL	Iterations	CFL	Iterations	CFL	Iterations	Cost(1)
Roe (1981)	0.5	9,652	0.9	1,155	0.6	1,921	0.0000706
Harten (1983)	0.5	5,371	0.9	1,175	0.6	1,684	0.0000789

(1): measured in seconds/per cell/per iteration

Table 5 shows the numerical data of the simulations performed with the Roe (1981) and the Harten (1983) schemes. As can be seen, the Harten (1983) scheme is more expensive than the Roe (1981) scheme (approximately 11.8% more expensive). However, the Harten (1983) scheme requires lower number of iterations to convergence than the Roe (1981) scheme in two of the three studied problems.

8. CONCLUSIONS

The present work performs comparisons between the Roe (1981) and the Harten (1983) algorithms applied to the solution of aeronautical and of aerospace problems, in two-dimensions. The Euler equations in conservative form, employing a finite volume formulation and an unstructured spatial discretization, are solved. The Roe (1981) and the Harten (1983) schemes are flux difference splitting ones and accurate solutions are expected. The time integration is performed by a Runge-Kutta method of five stages. Both schemes are first order accurate in space and second order accurate in time. The steady state physical problems of the transonic flow along a convergent-divergent nozzle and of the supersonic flows along a ramp and around a blunt body are studied. In all problems, the value of the entrance or attack angle is considered equal to zero. A spatially variable time step procedure is employed aiming to accelerate the convergence of the numerical schemes to the steady state solution. This technique has proved excellent gains in terms of convergence ratio as reported in Maciel (2005c).

The results have demonstrated that the Roe (1981) scheme yielded more severe pressure fields in the ramp and in the blunt body problems, while the Harten (1983) scheme yielded a more severe pressure field in the nozzle problem. The Harten (1983) scheme presented better wall pressure distribution in the nozzle problem, in comparison with the experimental data. In the ramp problem, both schemes presented similar behavior in the wall pressure distribution and in the prediction of the shock angle. The Roe (1981) scheme yielded better value to the stagnation pressure in the blunt body problem. In terms of computational cost, the Roe (1981) scheme is 11.8% cheaper than the Harten (1983) scheme.

9. REFERENCES

Anderson Jr., J. D., 1984, "Fundamentals of Aerodynamics", McGraw-Hill, Inc., EUA, 563p.

Frink, N. T., Parikh, P. and Pirzadeh, S., 1991, "Aerodynamic Analysis of Complex Configurations Using Unstructured Grids", AIAA 91-3292-CP.

Harten, A., 1983, "High Resolution Schemes for Hyperbolic Conservation Laws", Journal of Computational Physics, Vol. 49, pp. 357-393.

Jameson, A. and Mavriplis, D., 1986, "Finite Volume Solution of the Two-Dimensional Euler Equations on a Regular Triangular Mesh", AIAA Journal, Vol. 24, No. 4, pp. 611-618.

Kutler, P., 1975, "Computation of Three-Dimensional, Inviscid Supersonic Flows", Lecture Notes in Physics, Vol. 41, pp. 287-374.

Maciel, E. S. G., 2002, "Simulação Numérica de Escoamentos Supersônicos e Hipersônicos Utilizando Técnicas de Dinâmica dos Fluidos Computacional", Doctoral Thesis, ITA, CTA, São José dos Campos, SP, Brazil, 258 p.

Maciel, E. S. G., 2005a, "Comparison Between a Centered and a Flux Difference Split Schemes Using Unstructured Strategy", JBSMSE – Journal of the Brazilian Society of Mechanical Sciences and Engineering, Brazil, Vol. XXVII, No. 3, pp. 223-235.

Maciel, E. S. G., 2005b, "Comparison Between a Centered and a High Resolution Upwind Schemes in the Solution of Aerospace Problems Using Unstructured Strategy", Proceedings of the XVIII International Congress of Mechanical Engineering (XVIII COBEM), Ouro Preto, MG, Brazil.

Maciel, E. S. G., 2005c, "Analysis of Convergence Acceleration Techniques Used in Unstructured Algorithms in the Solution of Aeronautical Problems – Part I", Proceedings of the XVIII International Congress of Mechanical Engineering (XVIII COBEM), Ouro Preto, MG, Brazil.

Maciel, E. S. G., 2007, "Comparison Among Predictor-Corrector, Symmetrical and TVD Upwind Schemes in the Solution of the Euler Equations in Two-Dimensions – Theory", Proceedings of the XIX Congress of Mechanical Engineering (XIX COBEM), Brasília, DF, Brazil.

Mason, M. L., Putnam, L. E. and Re, R. J., 1980, "The Effect of Throat Contouring on Two-Dimensional Converging-Diverging Nozzles at Sonic Conditions", NASA Technical Paper 1704.

Mavriplis, D. J., 1990, "Accurate Multigrid Solution of the Euler Equations on Unstructured and Adaptive Meshes", AIAA Journal, Vol. 28, No. 2, pp. 213-221.

Pirzadeh, S., 1991, "Structured Background Grids for Generation of Unstructured Grids by Advancing Front Method", AIAA Paper 91-3233-CP.

Roe, P. L., 1981, "Approximate Riemann Solvers, Parameter Vectors, and Difference Schemes", Journal of Computational Physics, Vol. 43, pp. 357-372.

Steger, J. L., 1978, "Implicit Finite-Difference Simulation of Flow About Arbitrary Two-Dimensional Geometries", AIAA Journal, Vol. 16, No. 7, pp. 679-686.